

Article

Scenario-Based Stochastic Framework for Optimal Planning of Distribution Systems Including Renewable-Based DG Units

Ashraf Ramadan ¹, Mohamed Ebeed ² , Salah Kamel ¹ , Almoataz Y. Abdelaziz ³ and Hassan Haes Alhelou ^{4,*} 

¹ Department of Electrical Engineering, Faculty of Engineering, Aswan University, Aswan 81542, Egypt; ashraframadanragab@gmail.com (A.R.); skamel@aswu.edu.eg (S.K.)

² Department of Electrical Engineering, Faculty of Engineering, Sohag University, Sohag 82524, Egypt; mebeed@eng.sohag.edu.eg

³ Department of Electrical Engineering, Faculty of Engineering and Technology, Future University in Egypt, Cairo 11835, Egypt; almoataz.abdelaziz@fue.edu.eg

⁴ School of Electrical and Electronic Engineering, University College Dublin (UCD), Dublin 4, Ireland

* Correspondence: hassan.haesalhelou@ucd.ie

Abstract: Renewable energy-based distributed generators are widely embedded into distribution systems for several economical, technical, and environmental tasks. The main concern related to the renewable-based distributed generators, especially photovoltaic and wind turbine generators, is the continuous variations in their output powers due to variations in solar irradiance and wind speed, which leads to uncertainties in the power system. Therefore, the uncertainties of these resources should be considered for feasible planning. The main innovation of this paper is that it proposes an efficient stochastic framework for the optimal planning of distribution systems with optimal inclusion of renewable-based distributed generators, considering the uncertainties of load demands and the output powers of the distributed generators. The proposed stochastic framework depends upon the scenario-based method for modeling the uncertainties in distribution systems. In this framework, a multi-objective function is considered for optimal planning, including minimization of the expected total power loss, the total system voltage deviation, the total cost, and the total emissions, in addition to enhancing the expected total voltage stability. A novel efficient technique known as the Equilibrium Optimizer (EO) is actualized to appoint the ratings and locations of renewable-based distributed generators. The effectiveness of the proposed strategy is applied on an IEEE 69-bus network and a 94-bus practical distribution system situated in Portugal. The simulations verify the feasibility of the framework for optimal power planning. Additionally, the results show that the optimal integration of the photovoltaic and wind turbine generators using the proposed method leads to a reduction in the expected power losses, voltage deviations, cost, and emission rate and enhances the voltage stability by 60.95%, 37.09%, 2.91%, 70.66%, and 48.73%, respectively, in the 69-bus system, while in the 94-bus system these values are enhanced to be 48.38%, 39.73%, 57.06%, 76.42%, and 11.99%, respectively.

Keywords: renewable energy; uncertainties; distributed generators; wind turbine; solar photovoltaic; equilibrium optimizer; radial distribution system; scenario-based method



Citation: Ramadan, A.; Ebeed, M.; Kamel, S.; Abdelaziz, A.Y.; Haes Alhelou, H. Scenario-Based Stochastic Framework for Optimal Planning of Distribution Systems Including Renewable-Based DG Units. *Sustainability* **2021**, *13*, 3566. <https://doi.org/10.3390/su13063566>

Academic Editor:
Alberto-Jesus Perea-Moreno

Received: 2 March 2021
Accepted: 17 March 2021
Published: 23 March 2021

Publisher's Note: MDPI stays neutral with regard to jurisdictional claims in published maps and institutional affiliations.



Copyright: © 2021 by the authors. Licensee MDPI, Basel, Switzerland. This article is an open access article distributed under the terms and conditions of the Creative Commons Attribution (CC BY) license (<https://creativecommons.org/licenses/by/4.0/>).

1. Introduction

1.1. Problem Statement

Uncertainty is essential in the optimal power planning problem of electrical systems, and it is a main consideration adding to its complexity, specifically the uncertainties of the renewable energy resources (RERs) and load demands. Many research efforts related to the optimal integration of Distributed Generators (DGs) are expressed as ideal optimization problems, and only few have considered uncertainty. The optimal allocation of the photovoltaic (PV) and wind turbine (WT) units in power systems and techniques existing in the literature considering the uncertainty of systems have an incredible impact

on the planning of renewable DGs, and uncertainties effect the load demand and the output powers of solar and wind-based DGs in the distribution systems (DSs). The contribution and the research gap are referenced in detail. Electric power generation organizations will in general utilize (DGs) near the load to convey the electrical power to the consumers for technical, economic, and environmental reasons. As of late, integration of the RERs including wind and photovoltaic energies have become a favored solution for defeat increasing the load growth as they are sustainable and clean resources. Nonetheless, the inclusion of the RERs in the distribution grids face numerous issues due to their intermittency and the fluctuations of the output power, which increases the uncertainties in electrical systems. In this way, the uncertainties in power systems should be taken into consideration for correct planning and the secure operation of power systems.

1.2. Literature Survey

The essential purpose of efficient planning in distribution systems is to provide excellent solutions that guarantee the security, quality, and reliability of power supply to clients at the least cost [1]. The cost of power generation from conventional generators is expanding quickly because of the increase in fuel costs, although lately the generation cost of RERs has diminished. Alongside financial contemplations, another advantage of RERs is the eco-friendly power generation from these sources [2]. A stochastic scenario modeling of a multistage joint for the distribution systems planning has been utilized to decrease the operational and investment costs [3]. Sensible application of DGs can bring numerous points of interest, for example, voltage profile improvement, reducing emissions and energy cost [4–6].

Nonetheless, improper placement of DGs may lead to the fluctuations of voltage and also system instability because of the uncertain nature of RERs [7,8]. The issue of optimal integration of DGs has been explored in the several papers from different points of view. The authors in [9] suggested an improved adaptive genetic algorithm for resolving the optimal DG allocation problem. In [10], an efficient framework has been suggested for the optimal DG allocation problem to reduce the system costs. The authors in [11] offered a genetic algorithm along with the Monte Carlo method for solving the optimal DG integration problem under the uncertainties of RER generation. The cost of energy losses and DGs have been considered in the model. In [12], an efficient method has been presented for the optimal planning of accommodating the integration of PEV along with renewable DGs under uncertainties of the system. In [13], the optimal power planning problem in the active distribution system is solved to reduce total cost and emissions using a cuckoo search (CS) with optimal integration of WTs and demand response, considering the uncertainties of the system by the scenario synthesis method. The authors in [14] applied the Crisscross Optimization Algorithm and Monte Carlo Simulation for assigning the rating and location of DGs in the distribution system for reducing the power losses and the cost. Esmaeili et al. presented a multi-objective framework for optimizing the DG allocation and reconfiguration of the distribution network using the Big Bang–Big Crunch algorithm [15]. In [16], a probabilistic planning method was suggested based on mixed integer nonlinear programming (MINLP) and has been implemented to assign energy loss reduction with optimal integration of RERs in a rural distribution system. The author in [17] proposed a stochastic model for optimizing the investment of the DGs under uncertain conditions in distribution networks. Ref. [18] proposed a planning strategy for a hybrid solar-wind generation MG system with hydrogen energy storage using a novel multi-objective optimization algorithm to minimize the following three objective functions: loss of load expected, annualized cost of the system, and loss of energy expected. Ref. [19] proposed an algorithm for DG allocation planning based on using the probabilistic uncertainty modeling method. Several optimization algorithms have been used to determine the best size and location of DGs in a radial distribution network (RDN) considering the uncertainties of systems such as Particle Swarm Optimization (PSO) [20], modified sine cosine algorithm [21], Cuckoo Search Algorithm (CA) [22], water

cycle algorithm [23], Improved Antlion Optimization Algorithm (IALO) [24], Specialized Genetic Algorithm (SGA) [25], Ant Colony Optimizer (ACO) [26], Modified Differential Evolution Algorithm (MDEA) [27], harmony search algorithm [28], Seeker Optimization Algorithm (SOA) [29], and teaching learning-based optimization [30].

The Equilibrium Optimizer (EO) is a novel physical-based optimization technique which emulates the control volume mass balance models [31]. The EO has been applied for solving numerous engineering problems, and in [32] it has been applied for solving the economic dispatch of a micro-grid. The authors in [33] applied the EO for assigning the optimal rating and locations of the renewable-based DGs for loss reduction under uncertainties of the system. In [34], the EO was implemented for optimizing the structural design of vehicle components. The EO was employed for solving the optimal power flow problem in an AC/DC network. The solar photovoltaic parameters have been estimated using the EO in [35].

In this paper, the EO is utilized for deciding the best allocation of the solar and wind units for minimization of the expected power losses, the system voltage deviation, the total cost, and the total emissions as well as enhancing the expected voltage stability considering the uncertainties of load demands and solar and wind power generators in an IEEE 69-bus network and a 94-bus practical distribution system situated in Portugal.

1.3. Contribution of Paper

From the previous survey, the main concern or the problem statement related to the optimal planning of distribution systems with the inclusion of optimal RERs is the uncertainties of load demand and the output power of the RERs. Therefore, the planning problem became more complex and needs an efficient method to be solved.

This paper contributes to the existing body of knowledge as it solves the optimal planning problem in a distribution system for optimal incorporation of DGs using a scenario-based stochastic framework considering the uncertainties of load demands and the output powers of RERs. The innovation and contributions of this paper are summarized as follows:

- Proposing an efficient framework for the optimal planning of distribution systems considering the uncertainties of load and the output powers of renewable based DGs.
- The application of scenario-based methods for modeling the uncertainties in the electrical systems.
- The application of an efficient algorithm, called the EO, for solving the planning problem.
- The developed algorithms are applied for optimal integration of the renewable-based DGs for loss reduction, voltage improvements, system voltage deviation, the total cost, and the total emissions of the IEEE 69-bus and 94-bus distribution networks.
- A comparison is presented between the EO and other well know techniques for solving the planning problem.

1.4. Paper Layout

The paper is arranged as follows: Section 2 displays the problem formulation including the objective function. Section 3 illustrates the uncertainty modeling methods. Section 4 introduces an overview of the EO technique. Section 5 shows the obtained outcomes, while Section 6 lists the paper's conclusions.

2. Problem Formulation

In this study, five objective functions are considered in a multi-objective function. It is worth mentioning that in case of modeling or considering the uncertainties in power systems, a set of scenarios will be generated. Thus, these scenarios should be considered for the efficient solving of planning problems, and each scenario has its expected values as depicted in the following sections. In this work, the considered objective function is

a multi-objective function comprising five objective functions which can be presented as follows:

2.1. The Objective Functions

2.1.1. Minimization of the Expected Power Loss (EP_{Loss})

The expected power losses of the radial distribution network are determined as follows:

$$P_{loss(k,k+1)} = R_{k,k+1} \left(\frac{P_k^2 + jQ_k^2}{|V_k|^2} \right) \quad (1)$$

where

$$P_{Total_Loss} = \sum_{i=1}^{NT} P_{Loss,i} \quad (2)$$

$$ETP_{Loss} = \sum_{k=1}^{Ns} EP_{Loss,k} = \sum_{k=1}^{Ns} \pi_{S,k} \times P_{Total_Loss,k} \quad (3)$$

2.1.2. Minimization of the Expected Voltage Deviations ($ETVD$)

The expected summation of the voltage deviations of the radial distribution network are given as follows:

$$ETVD = \sum_{k=1}^{Ns} EVD_k = \sum_{k=1}^{Ns} \pi_{S,k} \times VD_k \quad (4)$$

where

$$VD = \sum_{n=1}^{NB} |V_n - 1| \quad (5)$$

2.1.3. Enhancement of the Expected Voltage Stability ($ETVSI$)

The expected summation of the voltage stability indices can be expressed as follows:

$$ETVSI = \sum_{k=1}^{Ns} EVSI_k = \sum_{k=1}^{Ns} \pi_{S,k} \times VSI_k \quad (6)$$

where

$$VSI_n = |V_n|^4 - 4(P_n X_{nm} - Q_n R_{nm})^2 - 4(P_n X_{nm} + Q_n R_{nm})|V_n|^2 \quad (7)$$

2.1.4. Minimization of the Expected Total Cost (ETC_{Cost})

The expected total annual cost (ETC_{Cost}) is considered, which consists of the expected annual energy loss cost ($ECost_{loss}$), the expected cost of the electric energy savings from the main substation ($ECost_{Grid}$), the expected PV units cost ($ECost_{PV}$), and the expected WT cost ($ECost_{WT}$). It can be represented as follows:

$$ETC_{Cost} = ECost_{loss} + ECost_{Grid} + ECost_{PV} + ECost_{WT} \quad (8)$$

The items detailed in Equation (8) are defined as follows:

$$Cost_{Grid} = 8760 \times K_{Grid} \times P_{Grid} \quad (9)$$

$$ETC_{Cost_{Grid}} = \sum_{k=1}^{Ns} ECost_{Grid,k} = \sum_{k=1}^{Ns} \pi_{S,k} \times Cost_{Grid,k} \quad (10)$$

$$Cost_{Loss} = 8760 \times K_{Loss} \times P_{Total_loss} \quad (11)$$

$$ETC_{Cost_{Loss}} = \sum_{k=1}^{Ns} ECost_{Loss,k} = \sum_{k=1}^{Ns} \pi_{S,k} \times Cost_{Loss,k} \quad (12)$$

$$ETCost_{wind} = \sum_{k=1}^{Ns} ECost_{wind,k} = \sum_{k=1}^{Ns} \pi_{S,k} \times (a_1 + 8760 \times b_1 \times P_{WT,k}) \quad (13)$$

$$a_1 = CF \times CSDG_{WT} \times P_{wr} \quad (14)$$

$$b_1 = Cost_{WT_{O\&M}} + Cost_{WT_{Fuel}} \quad (15)$$

$$CF = \frac{\rho \times (1 + \rho)^{NP}}{(1 + \rho)^{NP} - 1} \quad (16)$$

where a_1 is the annual installment of the wind turbine, and b_1 is the annual operation and maintenance cost of the wind turbine.

$$ETCost_{PV} = \sum_{k=1}^{Ns} ECost_{PV,k} = \sum_{n=1}^{Ns} \pi_{S,k} \times (a_2 + 8760 \times b_2 \times P_{PV,k}) \quad (17)$$

$$a_2 = CF \times CSDG_{PV} \times P_{sr} \quad (18)$$

$$b_2 = Cost_{PV_{O\&M}} + Cost_{PV_{Fuel}} \quad (19)$$

where a_2 is the annual installment of the PV unit, and b_2 is the annual operation and maintenance cost of the PV unit. In this paper the cost coefficients of PV are selected to be $CSDG_{PV} = 770$ USD/kW, $Cost_{PV_{O\&M}} = 0.01$ USD/kWh, $Cost_{PV_{Fuel}} = 0$ USD/kWh, and the cost coefficients of the wind are selected to be $CSDG_{WT} = 4000$ USD/kW, $Cost_{WT_{O\&M}} = 0.01$ USD/kWh, $Cost_{WT_{Fuel}} = 0$ USD/kWh [36].

2.1.5. Minimization of the Expected Total Emissions ($ETEmission$)

The expected total annual emissions in kilotons (Kt) can be expressed as follows:

$$ETEmission = \sum_{k=1}^{Ns} EEmission_k = \sum_{n=1}^{Ns} \pi_{S,k} \times P_{Grid,k} \times LF \times ER_{Grid} \times 8760 \quad (20)$$

According to ER_{Grid} , the emission rate of grid values of NO_x, CO₂, and SO₂ are 2.2952 kg/MWh, 921.25 kg/MWh and 3.5834 kg/MWh, respectively [15].

2.1.6. The Multi-Objective Function

In this work, the previous objective functions are considered simultaneously. To consider these objective functions concurrently, the weight approach method is utilized. In addition, the objectives should be normalized as follows via division by its base value (without PV or WT), which makes the objective function dimensionless and also prevents any scaling problems. The augmented objective function can be described as follows:

$$F = \alpha_1 F_1 + \alpha_2 F_2 + \alpha_3 F_3 + \alpha_4 F_4 + \alpha_5 F_5 \quad (21)$$

where α_1 , α_2 , α_3 , α_4 , and α_5 are weighting factors. The summation of weight factors should equal 1 as follows:

$$|\alpha_1| + |\alpha_2| + |\alpha_3| + |\alpha_4| + |\alpha_5| = 1 \quad (22)$$

The normalized objective functions can be formulated as follows:

$$F_1 = \frac{ETP_{Loss}}{ETP_{Loss_{base}}} \quad (23)$$

$$F_3 = \frac{ETVD}{ETVD_{base}} \quad (24)$$

$$F_5 = \frac{1}{ETVSI} \quad (25)$$

$$F_4 = \frac{ETCost}{ETCost_{base}} \quad (26)$$

$$F_5 = \frac{ETEmission}{ETEmission_{base}} \quad (27)$$

2.2. The System Constraints

The system constraints are categorized as follows:

2.2.1. Equality Constraints

$$P_{Grid} + \sum_{i=1}^{NPV} P_{PV,i} + \sum_{i=1}^{NWT} P_{WT,i} = \sum_{i=1}^{NT} P_{loss,i} + \sum_{i=1}^{NB} P_{L,i} \quad (28)$$

$$Q_{Grid} + \sum_{i=1}^{NT} Q_{WT,i} = \sum_{i=1}^{NT} Q_{loss,i} + \sum_{i=1}^{NB} Q_{L,i} \quad (29)$$

2.2.2. Inequality Constraints

$$V_{min} \leq V_i \leq V_{max} \quad (30)$$

$$\sum_{i=1}^{NWT} Q_{WT,i} \leq \sum_{i=1}^{NB} Q_{L,i} \quad (31)$$

$$I_n \leq I_{max,n} \quad n = 1, 2, 3, \dots, NT \quad (32)$$

3. Uncertainty Modeling

In this work, the uncertainties that existed in the power system are considered by solving the problem of optimal power planning. The proposed stochastic framework considered three uncertain parameters including load demand, solar irradiance, and wind speed. The continuous probability density functions (PDFs) of wind speed, solar irradiance, and loads are used for representing the uncertainties of these parameters; then, the scenario-based method is utilized for generating a set of scenarios from combinations of these parameters. The proposed stochastic framework can be depicted as follows:

3.1. Modeling of Load Demand

The normal PDF ($f_d(P_d)$) is used for uncertainty representation of the load demand, which can be described using the following equations [37]:

$$f_d(P_d) = \frac{1}{\sigma_d \sqrt{2\pi}} \exp \left[-\frac{(P_d - \mu_d)^2}{2\sigma_d^2} \right] \quad (33)$$

The generated load scenarios and their probabilities obtained from (33) can be obtained as follows [38]:

$$\pi_{d,i} = \int_{P_{d,i}^{min}}^{P_{d,i}^{max}} \frac{1}{\sigma_d \sqrt{2\pi}} \exp \left[-\frac{(P_d - \mu_d)^2}{2\sigma_d^2} \right] dP_d \quad (34)$$

$$P_{d,i} = \frac{1}{\tau_{d,i}} \int_{P_{d,i}^{min}}^{P_{d,i}^{max}} \frac{P_d}{\sigma_d \sqrt{2\pi}} \exp \left[-\frac{(P_d - \mu_d)^2}{2\sigma_d^2} \right] dP_d \quad (35)$$

In this work, three load scenarios are presented. The load scenarios are obtained by dividing the normal PDF into three intervals. Table 1 provides the load scenarios and their probabilities when μ_d and σ_d are 70 and 10 [39].

Table 1. The generated scenarios of the uncertain parameters.

Load Scenario	$\pi_{d,i}$	Loading %
1	0.1587	54.7486
2	0.6827	70.0000
3	0.1587	85.2514
Wind Scenario	$\pi_{wind,z}$	Wind Speed (m/s)
1	0.7902	7.4518
2	0.1694	13.6153
3	0.0404	17.7289
Irradiance Scenario	$\pi_{Solar,m}$	Solar Irradiance (W/m ²)
1	0.1605	416.0627
2	0.4412	609.1166
3	0.3983	790.4621

3.2. Modeling of Wind Speed

The Weibull PDFs ($f_v(v)$) are used to describe the uncertainties of wind speed which can be expressed as follows [38]:

$$f_v(v) = \left(\frac{k}{c}\right) \left(\frac{v}{c}\right)^{(k-1)} e^{-(v/c)^k} \quad 0 \leq v < \infty \quad (36)$$

The wind turbine output power can be specified as follows [40,41]:

$$P_w(v_\omega) = \begin{cases} 0 & \text{for } v_\omega < v_{\omega i} \text{ \& } v_\omega > v_{\omega o} \\ P_{wr} \left(\frac{v_{\omega o} - v_{\omega i}}{v_{wr} - v_{\omega i}} \right) & \text{for } (v_{\omega i} \leq v_\omega \leq v_{wr}) \\ P_{wr} & \text{for } (v_{wr} < v_\omega \leq v_{\omega o}) \end{cases} \quad (37)$$

Additionally, a set of scenarios can be obtained from (36) by dividing the $f_v(v)$ into of a set of wind speed intervals. The generated wind speeds and their probabilities can be obtained as follows [42]:

$$\pi_{wind,z} = \int_{v_z^{min}}^{v_z^{max}} \left(\left(\frac{k}{c}\right) \left(\frac{v}{c}\right)^{(k-1)} e^{-(v/c)^k} \right) dv \quad (38)$$

$$v_z = \frac{1}{\pi_{wind,z}} \int_{v_z^{min}}^{v_z^{max}} \left(\left(\frac{k}{c}\right) \left(\frac{v}{c}\right)^{(z-1)} e^{-(v/c)^z} \right) dv \quad (39)$$

In this paper, three scenarios of wind speed are generated from the previous equations. The wind speed scenarios and their probabilities are listed in Table 1 in the case of selecting c and k to be 10.0434 and 2.5034, respectively, as given in [38].

3.3. Modeling of Solar Irradiance

The Beta PDF is used to specify the uncertainty of the solar irradiance, which can be given as follows [43]:

$$f_G(G) = \begin{cases} \frac{\Gamma(\alpha+\beta)}{\Gamma(\alpha)\Gamma(\beta)} \times G^{\alpha-1} \\ \times (1-G)^{\beta-1} & \text{If } 0 \leq G \leq 1, 0 \leq \alpha, \beta \\ 0 & \text{otherwise} \end{cases} \quad (40)$$

$$\beta = (1 - \mu_s) \times \left(\frac{\mu_s \times (1 + \mu_s)}{\sigma_s^2} \right) - 1 \quad (41)$$

$$\sigma_s = (1 - \mu_s) \times \left(\frac{\mu_s \times \beta}{(1 - \mu_s)} \right) - 1 \quad (42)$$

The yield power from the PV system can be calculated as follows [44,45]:

$$P_s(G) = \begin{cases} P_{sr} \left(\frac{G^2}{G_{std} \times X_c} \right) & \text{for } 0 < G \leq X_c \\ P_{sr} \left(\frac{G}{G_{std}} \right) & \text{for } G \geq X_c \end{cases} \tag{43}$$

In the previous equation, G_{std} is set to be 1000 W/m^2 , and X_c is a certain irradiance point is set to be 120 W/m^2 [41]. Three scenarios can be obtained from the previous equations by dividing the PDF into three intervals. The portability of solar irradiance and its corresponding solar irradiance for each scenario are given as follows [42]:

$$\pi_{Solar,m} = \int_{G_m^{min}}^{G_m^{max}} f_G(G) dG \tag{44}$$

$$G_m = \frac{1}{\pi_{Solar,m}} \int_{G_m^{min}}^{G_m^{max}} \left(\frac{\Gamma(\alpha + \beta)}{\Gamma(\alpha) \cdot \Gamma(\beta)} \times G^{\alpha-1} \times (1 - G)^{\beta-1} \right) dG \tag{45}$$

The generated scenarios of the solar irradiance and their probabilities are listed in Table 1 in the case of selecting α and β to be 6.38 and 3.43, respectively, as given in [38].

3.4. The Combined Load-Generation Model

To consider the uncertainties of the load demand, wind speed, and irradiance simultaneously, the probabilities of these parameters depicted in (34), (38), and (44) are multiplied together according to (46) as follows:

$$\pi_S = \pi_{d,i} \times \pi_{wind,k} \times \pi_{Solar,m} \tag{46}$$

A total of 27 scenarios can be obtained from (46). Table 2 shows the obtained scenarios and the value of the uncertain parameters and their probabilities.

Table 2. The combined scenarios and their probabilities.

Scenario	Loading %	Wind Speed (m/s)	Solar Irradiance (W/m ²)	$\pi_{d,i}$	$\pi_{Solar,m}$	$\pi_{wind,z}$	π_S
S1	54.7486	7.4518	416.0627	0.1587	0.1605	0.7902	0.0201
S2	54.7486	13.6153	416.0627	0.1587	0.1605	0.1694	0.0043
S3	54.7486	17.7289	416.0627	0.1587	0.1605	0.0404	0.0010
S4	54.7486	7.4518	609.1166	0.1587	0.4412	0.7902	0.0553
S5	54.7486	13.6153	609.1166	0.1587	0.4412	0.1694	0.0119
S6	54.7486	17.7289	609.1166	0.1587	0.4412	0.0404	0.0028
S7	54.7486	7.4518	790.4621	0.1587	0.3983	0.7902	0.0499
S8	54.7486	13.6153	790.4621	0.1587	0.3983	0.1694	0.0107
S9	54.7486	17.7289	790.4621	0.1587	0.3983	0.0404	0.0026
S10	70.0000	7.4518	416.0627	0.6827	0.1605	0.7902	0.0866
S11	70.0000	13.6153	416.0627	0.6827	0.1605	0.1694	0.0186
S12	70.0000	17.7289	416.0627	0.6827	0.1605	0.0404	0.0044
S13	70.0000	7.4518	609.1166	0.6827	0.4412	0.7902	0.2380
S14	70.0000	13.6153	609.1166	0.6827	0.4412	0.1694	0.0510
S15	70.0000	17.7289	609.1166	0.6827	0.4412	0.0404	0.0122
S16	70.0000	7.4518	790.4621	0.6827	0.3983	0.7902	0.2149
S17	70.0000	13.6153	790.4621	0.6827	0.3983	0.1694	0.0461
S18	70.0000	17.7289	790.4621	0.6827	0.3983	0.0404	0.0110
S19	85.2514	7.4518	416.0627	0.1587	0.1605	0.7902	0.0201
S20	85.2514	13.6153	416.0627	0.1587	0.1605	0.1694	0.0043
S21	85.2514	17.7289	416.0627	0.1587	0.1605	0.0404	0.0010
S22	85.2514	7.4518	609.1166	0.1587	0.4412	0.7902	0.0553
S23	85.2514	13.6153	609.1166	0.1587	0.4412	0.1694	0.0119
S24	85.2514	17.7289	609.1166	0.1587	0.4412	0.0404	0.0028
S25	85.2514	7.4518	790.4621	0.1587	0.3983	0.7902	0.0499
S26	85.2514	13.6153	790.4621	0.1587	0.3983	0.1694	0.0107
S27	85.2514	17.7289	790.4621	0.1587	0.3983	0.0404	0.0026

4. Equilibrium Optimizer

The EO is a modern optimizer which simulates models of the control volume mass balance to describe the dynamic and equilibrium states. In the EO, the concentrations denote the positions or the locations, while the particles represent the search agents of the optimizer. The particles update their location randomly around a vector known as equilibrium candidates. In addition, the generation rate is utilized for boosting the exploration and exploitation of the optimizer [31]. The mass balanced equation is described according to Equation (47) as follows:

$$V \frac{dX}{dt} = DX_{eq} - QX + G \quad (47)$$

where $V \frac{dX}{dt}$ describes the rate of mass changing in a volume. X refers to the concentration, and V represents the control volume. Q denotes the flow rate. G denotes the mass generation rate. By integration and manipulation of Equation (47), it is formulated as follows:

$$X = X_{eq} + (C_0 - C_{eq}) \exp[-\lambda(t - t_0)] + \frac{G}{\lambda V} (1 - (\exp[-\lambda(t - t_0)])) \quad (48)$$

where $\lambda = \left(\frac{D}{V}\right)$. X_0 refers to the initial concentration, and t_0 is the initial start time.

The Steps of EO

Step 1: Initialization

The initial concentrations are generated randomly according to (49).

$$X_i^{initial} = X_{min} + rand_i (X_{max} - X_{min}) \quad i = 1, 2, \dots, n \quad (49)$$

where X_{max} is the upper boundary of the control variable, while X_{min} is its lower limit.

$rand$ is a random value in the range [0,1]. Then, the objective function is evaluated for each obtained concentration.

Step 2: Assignment of the Equilibrium Candidates

The concentrations will be sorted according to their objective functions. The best four concentrations and their average vector represent the equilibrium candidates or the pool vector (X_{pool}), which can be expressed using (50) the following:

$$X_{pool} = \{X_1, X_2, X_3, X_4, X_{avg}\} \quad (50)$$

where

$$X_{avg} = \frac{X_1 + X_2 + X_3 + X_4}{4} \quad (51)$$

Step 3: Updating of the concentrations

Two vectors (r, λ) are created randomly, and they are used to control the exponential factor (F) to update the concentrations according to the following equations:

$$F = L_1 \text{sign}(r - 0.5) \left[e^{-\lambda t} - 1 \right] \quad (52)$$

where

$$t = \left(1 - \frac{T}{T_{Max}} \right)^{\left(L_2 \frac{T}{T_{Max}} \right)} \quad (53)$$

where L_1 and L_2 are constant values, which equal 2 and 1, respectively. These values are employed to adjust the exponential factor. T_{Max} is the maximum number of iterations, T refers to the T -th iteration. It should be indicated here that a_1 is employed to control the exploration process, while a_2 is employed to control the exploitation phase. $\text{sign}(r - 0.5)$ can also control the exploration direction.

Step 4: Applying the generation rate

It worth mentioning here that the generation rate is a robust approach for exploitation enhancement, and it can be defined as follows:

$$G = G_0 e^{-k(t-t_0)} \quad (54)$$

where

$$G_0 = GCP (X_{pool} - \lambda X) \quad (55)$$

$$GCP = \begin{cases} 0.5 & r_1 r_2 \geq GP \\ 0 & r_2 < GP \end{cases} \quad (56)$$

where r_1 and r_2 refer to a random value in the range of [0,1]. GP is the probability of generation, which is utilized to control the participation probability of concentration where it is updated by the generation rate. When $GP = 1$, the generation rate will not participate in the optimization process, while when $GP = 0$, the generation rate will greatly participate in the process. If $GP = 0$, the generation rate offers an admirable balancing between the exploration and exploitation procedures. According to the mentioned steps, the updated equation can be described using Equation (57):

$$X = X_{pool} + (X - X_{pool}) \cdot F + \frac{G}{\lambda V} (1 - F) \quad (57)$$

Step 5: Adding memory saving.

The obtained solutions or concentration will be compared with the previous solution. It is worth mentioning here that the EO is proposed to solve the presented optimal planning problem, where the main advantages of the Equilibrium Optimizer lie in its ability to assign optimal solutions with higher efficiency (i.e., less computational time or fewer number of iterations) when compared with other optimization techniques, as well as its high simplicity in updating the algorithm structure and its controllability between the exploitation and exploration phases. Its related disadvantage is that it is very sensitive to its selected parameters. Figure 1 describes application of the EO for the solution of the optimal power planning problem.

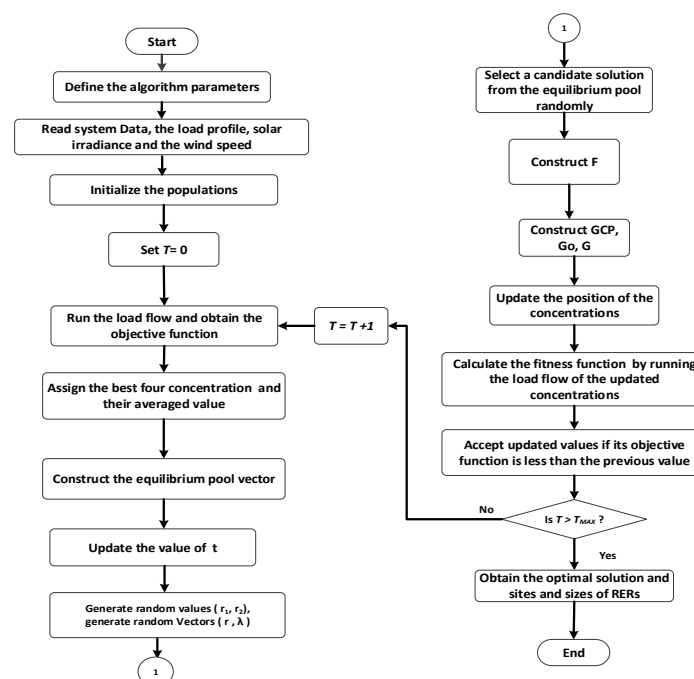


Figure 1. Application of the Equilibrium Optimizer (EO) for the optimal power planning solution.

5. Results and Discussion

The optimal power planning problem has been solved by the suggested algorithm (EO), and the optimal ratings and placement of wind turbines and solar PV units are assigned under the uncertainties of renewable energy and load demand. The objective function is a multi-objective function which comprises of (1) the expected power loss, (2) the expected summation of voltage deviations, (3) the expected voltage stability index, (4) the expected cost, and (5) the expected emissions. It should be highlighted here that the value of each weight factors in (21) is selected to be 0.2 for all studied cases. The EO algorithm is implemented for IEEE 69 and 94-bus systems, and the outcomes are compared with those obtained by the Sine Cosine Algorithm (SCA) [46], Particle Swarm Optimizer (PSO) [47], and the Anti Lion Algorithm (ALO) [48]. The single line diagram of the IEEE 69 and 94-bus systems are illustrated in Figures 2 and 3, respectively. The systems data of the 69-bus and 94-bus systems are given in [49,50], respectively. The system data and the initial load flow are provided in Table 3, while the constraints of the system are given in Table 4. The used parameters of the applied optimization techniques are tabulated in Table 5. It should be pointed out that the maximum number of search agents' and iterations or populations of the applied algorithms are selected to be the same for a fair comparison. The proposed EO technique as well as the other algorithms have been conducted on a I7-8700 CPU 3.2GHz and 24 GB RAM PC using MATLAB 2014a. The studied cases are presented below.

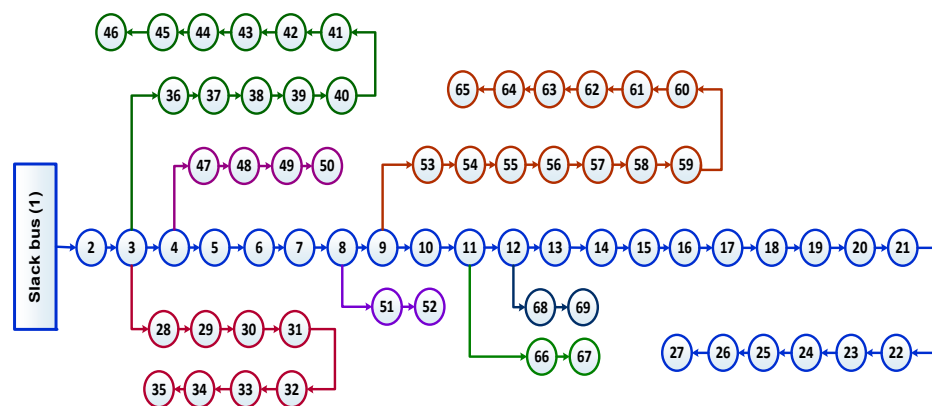


Figure 2. The IEEE 69-bus line diagram.

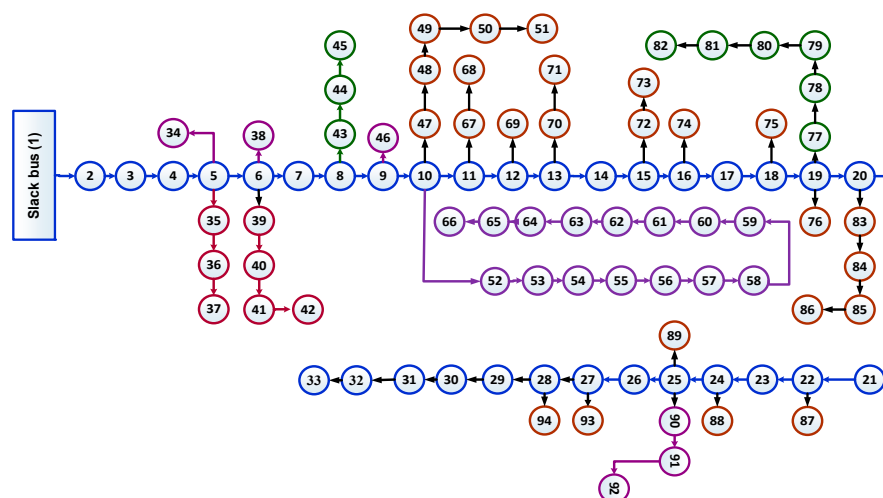


Figure 3. The IEEE 94-bus line diagram.

Table 3. The specifications of the studied systems and initial load flow solutions.

Item	69-Bus	94-Bus
System voltage	12.66 KV	15KV
V_{min} (p.u)	0.90919 @ bus 65	0.84749 @ bus 92
V_{max} (p.u) excluding the slack bus	0.99997 @ bus 2	0.99508 @ bus 2
Total active load demand (KW)	3801.490	4797.000
Total reactive load demand (KVAR)	2694.600	2323.900
Total active loss (KW)	224.975	365.173
Total reactive loss (KVAR)	102.187	505.785

Table 4. The system constraints.

Parameter	Value
Voltage limits	$0.90 \leq V_i \leq 1.05$ p.u
PV sizing limits for the 69-bus system	$0 \leq P_{PV} \leq 3801.490$ kW
WT sizing limits for the 69-bus system	$0 \leq P_{WT} \leq 3801.490$ kW
Power factor limits	$0.65 \leq PF_i \leq 1$
PV sizing limits for the 94-bus system	$0 \leq P_{PV} \leq 4797$ kW
WT sizing limits for the 94-bus system	$0 \leq P_{WT} \leq 4797$ kW

Table 5. The selected parameters of the optimization algorithms.

Algorithm	Parameter Settings
EO	$T_{max} = 100$, Search agents No. = 25, L1 = 2, L2 = 1, GP = 0.5
PSO	$T_{max} = 100$, Search agents No. = 25,
ALO	$T_{max} = 100$, Search agents No. = 25
SCA	$T_{max} = 100$, Search agents No. = 25

5.1. The IEEE 69-Bus System

The proposed algorithm is utilized to solve the optimal planning of the 69-bus system with optimal integration of RERs considering the uncertainties of the system. Initially, without integration of RERs, the total of the expected values of the power losses (ETP_{Loss}), the total of the expected values of the voltage deviations ($ETVD$), the total of the expected values of the voltage stability index ($ETVSI$), the expected values of the total cost (ETC_{Cost}), and the expected values of the emissions ($ETE_{Emission}$) are 144.0507 kW, 1.4014 p.u, 62.7261 p.u, 2,434,700 USD, and 15.947×10^3 kg/MWh, respectively. As mentioned, in Section 3, by combining the load demand, wind speed, and solar irradiance uncertainties, 27 scenarios have been generated to model the uncertainties of the system as depicted in Table 2. By application of the EO, the optimal sites for PV and wind turbine-based DGs are at buses number 26 and 62, respectively, while the optimal rating of the PV and wind turbine-based DGs are 177.5 kW and 1151 kW, respectively. Table 6 and Figure 4 provide the output power of the PV and wind turbine-based DGs for each scenario, as well as the corresponding P_{Loss} (MW), VD (pu), VSI (pu), $Cost$ (USD), and $Emission$ (kg/MWh). As solar irradiance, wind speed, and load demand have different values in each scenario, the yielded result will also be different. At a high probability value which occurred in scenario 13, according to Table 2 the output power of the wind turbine and PV systems is 394.2 kW and 108.4228 kW, respectively. Table 7 provides the expected values for each scenario with optimal integration of RERs. According to Table 7, the summation of the expected values including ETP_{Loss} , $ETVD$, $ETVSI$, ETC_{Cost} and $ETE_{Emission}$ are enhanced to be 56.2394 kW, 0.8816 p.u, 64.6087 p.u, 1,248,050 USD, and $4,677.936 \times 10^3$ kg/MWh, respectively.

Table 6. The output powers of renewable energy resources (RERs), the power losses, Voltage Deviations (VD), Voltage Stability Index (VSI), cost, and emission rates for each scenario of IEEE 69-bus system.

Scenario	P_w (kW)	P_{5_s} (kW)	P_{Loss} (MW)	π_s	VD (pu)	VSI (pu)	Cost (USD)	EEmission (kg/MWh)
S1	394.2	74.0592	48.4097	0.0201	0.8028	64.8894	1,071,600	345.9392
S2	939.9	74.0592	12.7234	0.0043	0.3889	66.4681	1,589,600	723.2575
S3	1151	74.0592	12.7201	0.0010	0.318	67.0724	1,785,600	860.2859
S4	394.2	108.4228	47.6489	0.0553	0.7733	65.0009	1,103,800	368.7346
S5	939.9	108.4228	12.2143	0.0119	0.3597	66.581	1,621,700	745.8896
S6	1151	108.4228	12.2965	0.0028	0.2924	67.1859	1,817,700	882.8625
S7	394.2	140.7023	47.0604	0.0499	0.7456	65.1057	1,133,900	390.0656
S8	939.9	140.7023	11.8596	0.0107	0.3323	66.687	1,651,700	767.0688
S9	1151	140.7023	12.0212	0.0026	0.2684	67.2924	1,847,700	903.9902
S10	394.2	74.0592	66.5655	0.0866	1.0111	64.119	1,090,700	353.3142
S11	939.9	74.0592	18.8061	0.0186	0.5899	65.6923	1,612,500	738.4678
S12	1151	74.0592	14.7628	0.0044	0.4346	66.2941	1,809,800	878.1181
S13	394.2	108.4228	65.433	0.2380	0.9813	64.23	1,123,000	376.3508
S14	939.9	108.4228	17.9418	0.0510	0.5603	65.8046	1,644,700	761.3304
S15	1151	108.4228	13.9894	0.0122	0.4051	66.407	1,842,000	900.9217
S16	394.2	140.7023	64.4987	0.2149	0.9534	64.3342	1,153,200	397.9062
S17	939.9	140.7023	17.2566	0.0461	0.5327	65.9101	1,674,900	782.7241
S18	1151	140.7023	13.3886	0.0110	0.3775	66.513	1,872,100	922.2607
S19	394.2	74.0592	91.9413	0.0201	1.2233	63.3491	1,114,300	361.2603
S20	939.9	74.0592	31.2589	0.0043	0.7942	64.9174	1,640,200	754.8008
S21	1151	74.0592	22.9091	0.0010	0.6363	65.5169	1,838,900	897.2459
S22	394.2	108.4228	90.4229	0.0553	1.1932	63.4595	1,146,700	384.5473
S23	939.9	108.4228	30.0269	0.0119	0.7644	65.0292	1,672,500	777.902
S24	1151	108.4228	21.7739	0.0028	0.6065	65.6292	1,871,200	920.2843
S25	394.2	140.7023	89.1295	0.0499	1.165	63.5631	1,177,100	406.3358
S26	939.9	140.7023	28.9996	0.0107	0.7365	65.1342	1,702,800	799.5178
S27	1151	140.7023	20.8364	0.0026	0.5787	65.7347	1,901,400	941.8418

Table 7. The expected values for each scenario of IEEE 69-bus system.

Scenario	π_s	ETP _{Loss} (pu)	ETVD (pu)	ETVSI (pu)	ETCost (USD)	ETEmission (kg/MWh)
S1	0.0201	0.973	0.0161	1.3043	21,540	6.9534
S2	0.0043	0.0547	0.0017	0.2858	6840	3.1100
S3	0.0010	0.0127	0.0003	0.0671	1790	0.8603
S4	0.0553	2.635	0.0428	3.5946	61,040	20.3910
S5	0.0119	0.1453	0.0043	0.7923	19,300	8.8761
S6	0.0028	0.0344	0.0008	0.1881	5090	2.4720
S7	0.0499	2.3483	0.0372	3.2488	56,580	19.4643
S8	0.0107	0.1269	0.0036	0.7136	17,670	8.2076
S9	0.0026	0.0313	0.0007	0.175	4800	2.3504
S10	0.0866	5.7646	0.0876	5.5527	94,460	30.5970
S11	0.0186	0.3498	0.011	1.2219	29,990	13.7355
S12	0.0044	0.065	0.0019	0.2917	7960	3.8637
S13	0.2380	15.573	0.2335	15.2867	267,270	89.5715
S14	0.0510	0.915	0.0286	3.356	83,880	38.8278
S15	0.0122	0.1707	0.0049	0.8102	22,470	10.9912
S16	0.2149	13.8608	0.2049	13.8254	247,830	85.5101
S17	0.0461	0.7955	0.0246	3.0385	77,210	36.0836
S18	0.0110	0.1473	0.0042	0.7316	20,590	10.1449
S19	0.0201	1.848	0.0246	1.2733	22,400	7.2613
S20	0.0043	0.1344	0.0034	0.2791	7050	3.2456
S21	0.0010	0.0229	0.0006	0.0655	1840	0.8972
S22	0.0553	5.0004	0.066	3.5093	63,410	21.2655
S23	0.0119	0.3573	0.0091	0.7738	19,900	9.2570
S24	0.0028	0.061	0.0017	0.1838	5240	2.5768
S25	0.0499	4.4476	0.0581	3.1718	58,740	20.2762
S26	0.0107	0.3103	0.0079	0.6969	18,220	8.5548
S27	0.0026	0.0542	0.0015	0.1709	4940	2.4488
Summation	1	56.2394	0.8816	64.6087	1,248,050	467.7936

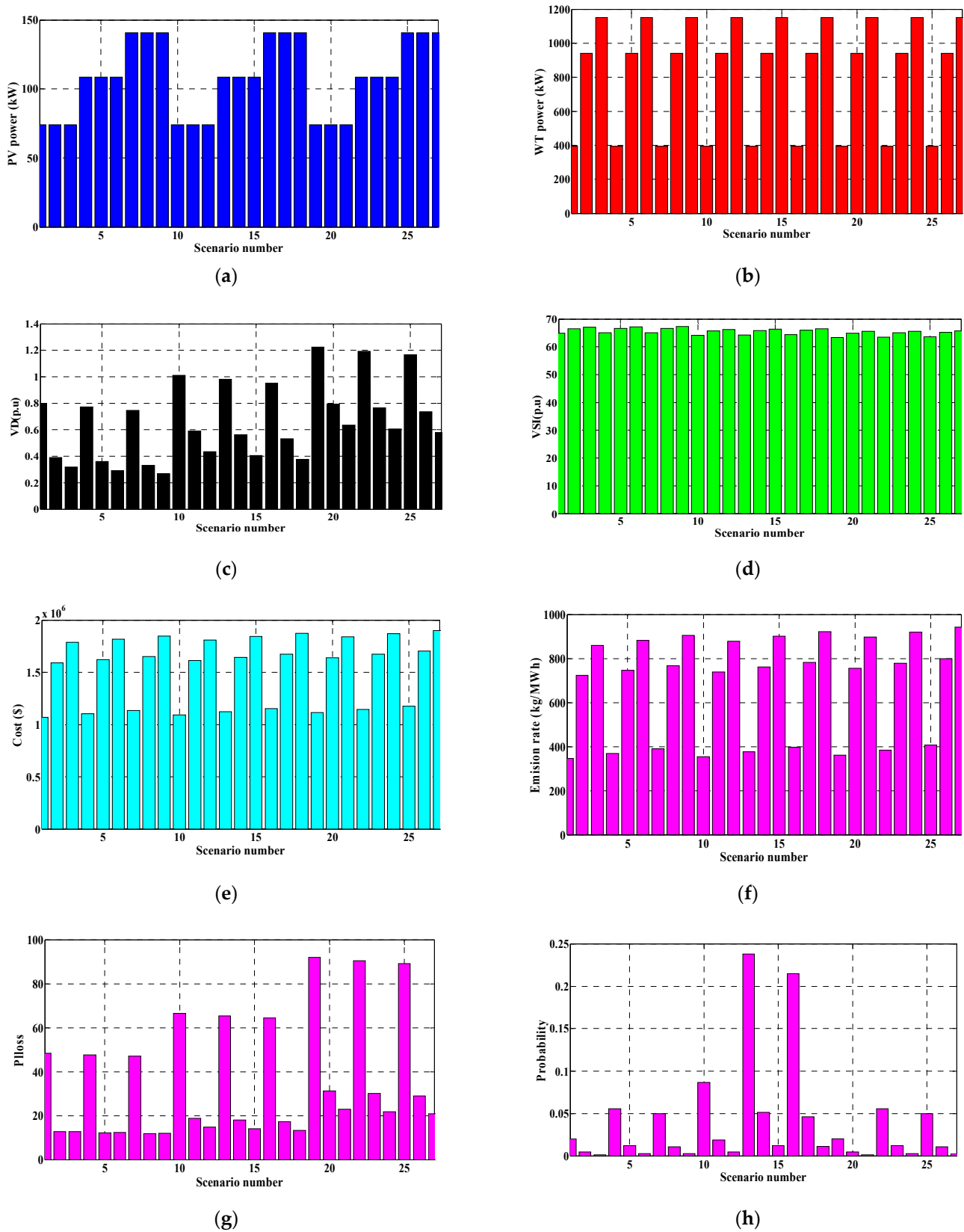


Figure 4. The outcomes for each scenario of the IEEE 69-bus system: (a) the photovoltaic (PV) power, (b) the wind turbine (WT) power, (c) the voltage deviations, (d) the voltage stability index, (e) the total cost, (f) the total emission rate, (g) the power loss, and (h) the probability.

In other words, the enhancement in the summation of the expected values with optimal integration of the RERs including ETP_{Loss} , $ETVD$, $ETVSI$, $ETCost$, and $ETEmission$ are 60.95%, 37.09%, 2.91%, 48.73%, and 70.66%, respectively. Figure 5 shows the voltage profile for the obtained scenarios. From this figure, it is obvious that the voltage magnitudes of all scenarios are within the allowable limits, and there is no violation which occurred. Table 8 shows a comparison of the obtained results by the application of other algorithms for the IEEE 69-bus system. Judging from Table 8, the minimum objective function has been obtained by the application of the EO compared with SCA, ALO, and PSO.

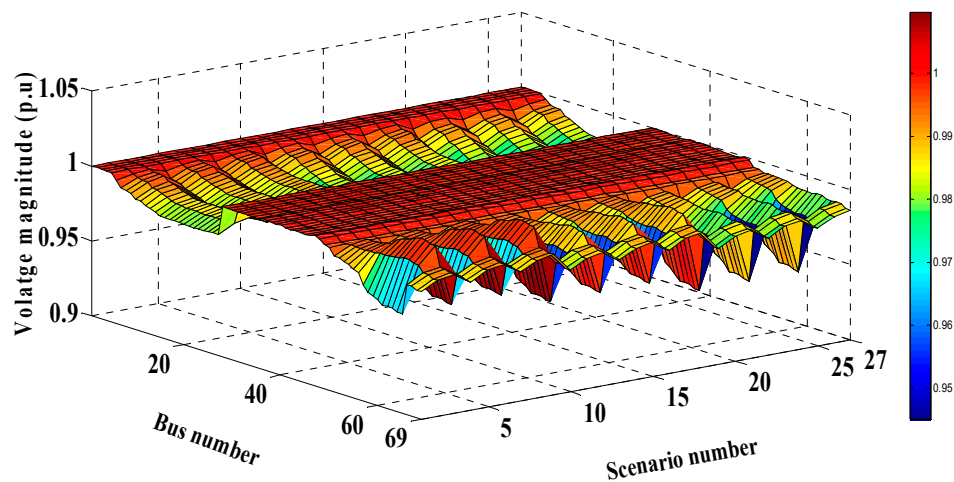


Figure 5. Voltage profile for each scenario of the 69-bus system.

Table 8. A comparison of the obtained results by the application of the investigated algorithms for the IEEE 69-bus system.

Algorithm	Average	Best Solution	Worst Solution	Standard Deviation
SCA	0.3660	0.3621	0.3851	0.0077
PSO	0.3934	0.3617	0.4505	0.0290
ALO	0.3928	0.3636	0.4147	0.0194
EO	0.3616	0.3609	0.3624	0.0006

5.2. The IEEE 94-Bus System

The optimal planning of the 94-bus system with the optimal integration of RERs considering the uncertainties of the system has been solved by the proposed algorithm. Initially, without the integration of RERs, the total of the expected values of the power losses (ETP_{Loss}), the total of the expected values of the voltage deviations ($ETVD$), the total of the expected values of the voltage stability index ($ETVSI$), the expected values of the total cost ($ETCost$), and the expected values of the emissions ($ETEmission$) are 204.6913 kW, 7.2162 p.u., 67.8052 p.u., 3,103,600 USD, and $20,254 \times 103$ kg/MWh, respectively. As referenced in Section 3, by combining load demand, wind speed, and solar irradiance uncertainties, 27 scenarios have been generated to model the uncertainties of the system as shown in Table 2. By utilization of the EO, the optimal sites for PV and wind turbine-based DGs are at buses number 91 and 23, respectively, while the optimal rating of the PV and wind turbine-based DGs are 107.5 kW and 1261.6 kW, respectively. Table 9 and Figure 6 provide the output power of the PV and wind turbine-based DGs for each scenario, as well as the corresponding P_{Loss} (MW), VD (pu), VSI (pu), $Cost$ (USD), and $Emission$ (kg/MWh). As solar irradiance, wind speed, and load demand have different values in each scenario, the yielded result will also be different. At a high probability value which occurred in scenario 13 according to Table 2, the output power of the wind turbine and PV systems are 432.2 kW and 65.1755 kW, respectively.

Table 9. The output powers of RERs, the power losses, Voltage Deviations (VD), Voltage Stability Index (VSI), cost, and emission rates for each scenario of the IEEE 94-bus system.

Scenario	P_w (kW)	P_s (kW)	P_{Loss} (MW)	π_s	VD (pu)	VSI (pu)	Cost (USD)	Emission (kg/MWh)
S1	432.2	44.5187	74.0228	0.0201	4.1453	77.6061	1,144,200	355.6937
S2	1030.5	44.5187	52.827	0.0043	1.5785	86.8996	1,706,500	757.7621
S3	1262	44.5187	62.2786	0.0010	1.2001	90.5301	1,918,400	901.8688
S4	432.2	65.1755	72.9507	0.0553	4.0964	77.7732	1,163,700	369.7955
S5	1030.5	65.1755	52.801	0.0119	1.5339	87.0723	1,725,600	771.1849
S6	1262	65.1755	62.5802	0.0028	1.207	90.705	1,937,500	915.0791
S7	432.2	84.5794	72.0738	0.0499	4.0507	77.9294	1,182,000	382.9575
S8	1030.5	84.5794	52.8868	0.0107	1.5015	87.2339	1,743,600	783.7222
S9	1262	84.5794	62.9677	0.0026	1.2138	90.8688	1,955,400	927.4206
S10	432.2	44.5187	112.9715	0.0866	4.987	74.7688	1,179,600	367.2078
S11	1030.5	44.5187	75.2483	0.0186	2.3577	83.974	1,747,100	780.0024
S12	1262	44.5187	79.4775	0.0044	1.453	87.5682	1,960,700	927.4984
S13	432.2	65.1755	111.2094	0.2380	4.9359	74.9366	1,199,300	381.7574
S14	1030.5	65.1755	74.644	0.0510	2.3114	84.1472	1,766,400	793.8006
S15	1262	65.1755	79.2327	0.0122	1.4557	87.7437	1,979,900	941.0633
S16	432.2	84.5794	109.6941	0.2149	4.8884	75.0935	1,217,800	395.3338
S17	1030.5	84.5794	74.1937	0.0461	2.2683	84.3093	1,784,600	806.6858
S18	1262	84.5794	79.1134	0.0110	1.4596	87.9079	1,998,000	953.7337
S19	432.2	44.5187	166.2304	0.0201	5.8647	71.9096	1,224,200	380.0133
S20	1030.5	44.5187	110.2486	0.0043	3.1668	81.0279	1,797,400	804.6575
S21	1262	44.5187	108.7544	0.0010	2.1969	84.586	2,012,800	955.8679
S22	432.2	65.1755	163.7147	0.0553	5.8113	72.0782	1,244,100	395.052
S23	1030.5	65.1755	109.0211	0.0119	3.1187	81.2017	1,817,000	818.8602
S24	1262	65.1755	107.9232	0.0028	2.1504	84.762	2,032,300	969.8134
S25	432.2	84.5794	161.5027	0.0499	5.7616	72.2358	1,262,900	409.0805
S26	1030.5	84.5794	107.9934	0.0107	3.0738	81.3643	1,835,300	832.1201
S27	1262	84.5794	107.2602	0.0026	2.107	84.9267	2,050,500	982.8367

Table 10 provides the expected values for each scenario with the optimal integration of RERs. According to Table 10, the summation of the expected values including ETP_{Loss} , $ETVD$, $ETVSI$, $ETCost$, and $ETEmission$ are enhanced to be 105.6493 kW, 4.3489 p.u., 77.0479 p.u., 1,332,680 USD, and 4774.689×10^3 kg/MWh, respectively. In other words, the enhancement in the summation of the expected values with optimal integration of the RERs including EP_{Loss} , EVD , $ETVSI$, $ETCost$, and $Emission$ are 48.38, 39.73%, 11.99%, 57.06%, and 76.42%, respectively. Figure 7 shows the voltage profile for the obtained scenarios.

Table 10. The expected values for each scenario of the 94-bus system.

Scenario	π_s	ETP_{Loss} (kW)	$ETVD$ (pu)	$ETVSI$ (pu)	$ETCost$ (USD)	$ETEmission$ (kg/MWh)
S1	0.0201	1.4879	0.0833	1.5599	23,000	71,494
S2	0.0043	0.2272	0.0068	0.3737	7340	32,584
S3	0.0010	0.0623	0.0012	0.0905	1920	9019
S4	0.0553	4.0342	0.2265	4.3009	64,350	204,497
S5	0.0119	0.6283	0.0183	1.0362	20,540	91,771
S6	0.0028	0.1752	0.0034	0.254	5430	25,622
S7	0.0499	3.5965	0.2021	3.8887	58,980	191,096
S8	0.0107	0.5659	0.0161	0.9334	18,660	83,858
S9	0.0026	0.1637	0.0032	0.2363	5080	24,113
S10	0.0866	9.7833	0.4319	6.475	102,150	318,002
S11	0.0186	1.3996	0.0439	1.5619	3,2500	145,080
S12	0.0044	0.3497	0.0064	0.3853	8630	40,810
S13	0.2380	26.4678	1.1748	17.8349	285,440	908,583
S14	0.0510	3.8068	0.1179	4.2915	90,090	404,838
S15	0.0122	0.9666	0.0178	1.0705	24,160	114,810
S16	0.2149	23.5733	1.0505	16.1376	261,710	849,572
S17	0.0461	3.4203	0.1046	3.8867	82,270	371,882
S18	0.0110	0.8702	0.0161	0.967	21,980	104,911
S19	0.0201	3.3412	0.1179	1.4454	24,610	76,383
S20	0.0043	0.4741	0.0136	0.3484	7730	34,600
S21	0.0010	0.1088	0.0022	0.0846	2010	9559
S22	0.0553	9.0534	0.3214	3.9859	68,800	218,464
S23	0.0119	1.2974	0.0371	0.9663	21,620	97,444
S24	0.0028	0.3022	0.006	0.2373	5690	27,155
S25	0.0499	8.059	0.2875	3.6046	63,020	204,131
S26	0.0107	1.1555	0.0329	0.8706	19,640	89,037
S27	0.0026	0.2789	0.0055	0.2208	5330	25,554
Summation	1	105.6493	4.3489	77.0479	1,332,680	4,774,869

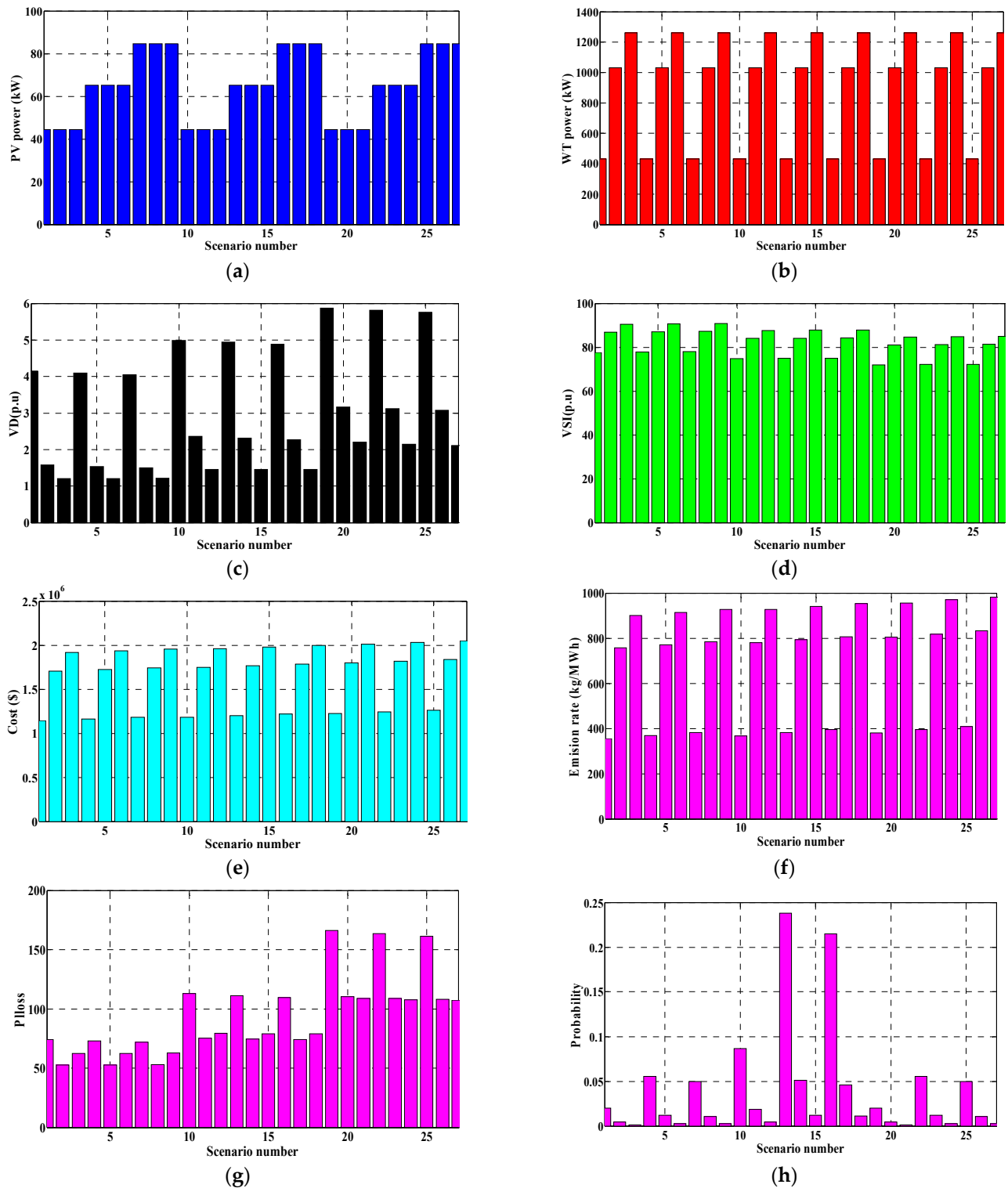


Figure 6. The outcomes for each scenario of the 94-bus system: (a) the PV power, (b) the WT power, (c) the voltage deviations, (d) the voltage stability index, (e) the total cost, (f) the total emission rate, (g) the power loss, and (h) the probability.

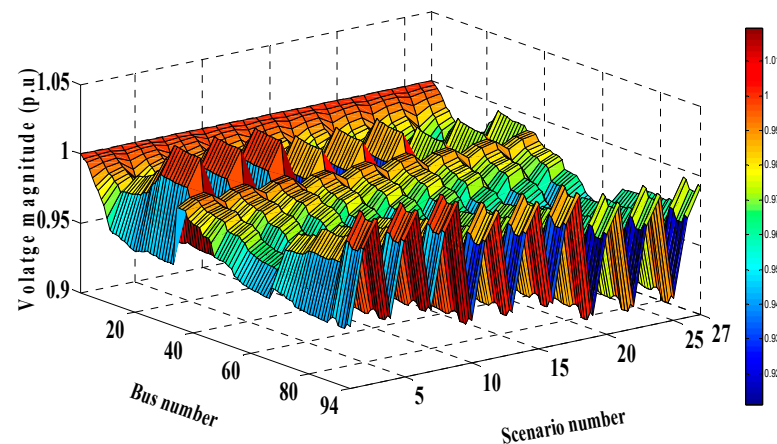


Figure 7. Voltage profile for each scenario of the 94-bus system.

From this figure, it is obvious that the voltage magnitudes of all scenarios are within the allowable limits, and no violation occurred. Table 11 shows a comparison of the obtained results by the application of other algorithms for the 94-bus system. Judging from Table 11, the minimum objective function has been obtained by the application of the EO compared with SCA, ALO, and PSO.

Table 11. A comparison of the obtained results by the application of the investigated algorithms on the 94-bus system.

Algorithm	Average	Best Solution	Worst Solution	SD
SCA	0.3546	0.3543	0.3562	0.0005
PSO	0.3738	0.3621	0.4141	0.0160
ALO	0.3898	0.3544	0.4879	0.0424
EO	0.3543	0.3535	0.3564	0.0008

6. Conclusions

In this paper, the optimal planning for distribution systems has been solved using an efficient stochastic framework by assigning the optimal sites and sizes of solar PV and wind turbine-based DGs under uncertainties of load demands, wind speeds, and solar radiation. The proposed framework is based on application of the Equilibrium Optimizer (EO) and the scenario-based method for reducing the expected power loss, the expected system voltage deviations, the expected total cost, the expected total emissions, and maximizing the expected voltage stability. The EO has been applied for solving the allocation problem of solar PV and wind turbine-based DGs, while the scenario-based method was utilized to represent the combination the uncertainties of load demands, wind speeds, and solar radiation. The proposed technique has been implemented on an IEEE 69-bus and 94-bus practical distribution system located in Portugal, and the obtained results were compared with those obtained by SCA, PSO, and ALO. The obtain results verified the following:

- The effectiveness of the proposed framework for solving the optimal planning problem for distribution systems.
- The superiority of the EO for assigning the optimal placement and sizes of the DGs compared to SCA, PSO, and ALO techniques.
- The inclusion of solar PV and wind turbine-based DGs using the proposed method in the IEEE 69-bus system can reduce the expected power losses, voltage deviations, cost, and emissions rate and enhance the voltage stability compared to the base case by 60.95%, 37.09%, 2.91%, 70.66%, and 48.73%, respectively.
- The inclusion of solar PV and wind turbine-based DGs using the proposed method in a 94-bus system can reduce the expected power losses, voltage deviations, cost, and

emissions rate and enhance the voltage stability compared to the base case by 48.38%, 39.73%, 57.06%, 76.42%, and 11.99%, respectively.

Author Contributions: Conceptualization, A.R., M.E., S.K., H.H.A.; data curation, A.Y.A.; formal analysis, A.R. and M.E.; resources, A.Y.A.; methodology, S.K.; software, A.R., M.E. and S.K.; supervision, A.Y.A., H.H.A.; validation, A.R. and S.K.; visualization, A.Y.A.; writing—original draft, A.R. and M.E.; writing—review and editing, S.K., H.H.A. and A.Y.A. All authors together organized and refined the manuscript in the present form. All authors have approved the final version of the submitted paper. All authors have read and agreed to the published version of the manuscript.

Funding: H. Haes Alhelou was supported in part by Science Foundation Ireland (SFI) under the SFI Strategic Partnership Programme Grant Number SFI/15/SPP/E3125 and additional funding provided by the UCD Energy Institute. The opinions, findings, and conclusions or recommendations expressed in this material are those of the authors and do not necessarily reflect the views of the Science Foundation Ireland.

Institutional Review Board Statement: Not applicable.

Informed Consent Statement: Not applicable.

Data Availability Statement: Not applicable.

Conflicts of Interest: The authors declare no conflict of interest.

Abbreviations

Acronyms

DGs	Distributed Generators
DSs	Distribution Systems
PV	Photovoltaic
WT	Wind Turbine
RERs	Renewable Energy Resources
PDF	Probability Distribution Function
RDN	Radial Distribution Network
EO	Equilibrium Optimizer
SCA	Sine Cosine Algorithm
ALO	Ant-Lion Optimizer
PSO	Particle Swarm Optimization
IAGA	Improved Adaptive Genetic Algorithm
MFO	Moth Flame Optimization
GA	Genetic-Algorithm
GA-MCS	Genetic-Algorithm with Monte Carlo simulation
CSA	Cuckoo Search Algorithm
CSO-MCS	Crisscross Optimization Algorithm and Monte Carlo Simulation
IALO	Improved Antlion Optimization Algorithm
SGA	Specialized Genetic Algorithm
ACO	Ant Colony Optimizer
MDEA	Modified Differential Evolution Algorithm
SOA	Seeker Optimization Algorithm

Indices and Sets

P_{loss}	Loss power
P_{Total_Loss}	The total active power loss
ETP_{Loss}	Expected Total Loss Power
$R_{k,k+1}$	The resistance of the line between buses k and $k + 1$,
P_k	Real power
Q_k	Reactive powers
P_L	The active load demand

Q_L	The reactive load demand
V_k	Nominal voltage
$EP_{Loss,k}$	Expected power loss for scenario k
ETP_{Loss}	Expected total power loss
VD	Voltage Deviations
EVD_k	Expected voltage deviation for scenario k
$ETVD$	Expected total voltage deviation
VSI	Voltage Stability Index
$EVSI_k$	Expected Voltage Stability Index for scenario k
$ETVSI$	Expected total Voltage Stability Index
$EEmission_k$	Expected emission for scenario k
$ETEmission$	Expected total emission
NB	Number of buses
Kt	Kilotons
PF	Power Factor
$ECost_{Grid,k}$	Expected cost grid for scenario k
$ETCost_{Grid}$	Expected total cost grid
$ECost_{Loss,k}$	Expected cost loss for scenario k
$ETCost_{Loss}$	Expected total cost loss
$ECost_{wind,k}$	Expected cost wind for scenario k
$ETCost_{wind}$	Expected total cost wind
$ECost_{PV,k}$	Expected cost solar for scenario k
$ETCost_{PV}$	Expected total cost solar
$TVSI$	Total Voltage Stability Index
$ETVSI$	Expected Total Voltage Stability Index
$ETCost$	The expected total annual cost
$ECost_{loss}$	The expected annual energy loss cost
$Cost_{Grid}$	Cost of the power injection at substation
$ECost_{Grid}$	The expected cost of the power injection at substation
$ECost_{PV}$	The expected PV units cost
P_{Grid}	Power of the grid
K_{Grid}	Cost of electricity in USD/kW h
$Cost_{Loss}$	Cost of the losses
K_{Loss}	The energy loss cost
P_{Total_loss}	The total power losses
$ECost_{Loss}$	The expected loss cost
π_S	The Combined probabilities
$\pi_{d,i}$	The portability of load demand of i -th interval
$\pi_{wind,z}$	The probability of the wind speed of z -th interval
$\pi_{Solar,m}$	The probability of the solar irradiance of m -th interval
$ECost_{wind}$	The expected WT cost
CF	The capital recovery factor
P_{wr}	Rated output power of the WT
$ECost_{PV}$	The expected PV cost
$CSDG_{PV}$	Installation cost of the PV
P_{sr}	The rated power of PV unit
P_s	The output power of PV unit
P_{wr}	The rated power of WT
P_w	The output power of WT
$Cost_{PV_{O\&M}}$	Operation and maintenance costs of the PV unit
$CSDG_{wind}$	Installation cost of the WT
$Cost_{WT_{O\&M}}$	Operation and maintenance costs of the WT
ER_{Grid}	The emission rate of grid
LF	Load factor
$ETP_{Loss_{base}}$	Expected Total power loss of base case
$ETVD_{base}$	Expected voltage deviation of base case
$ETCost_{base}$	Expected total cost of base case

$ETEmission_{base}$	Expected emission rate of base case
f_d	The normal PDF of load demand
f_v	The Weibull PDF of wind speed
f_G	The Beta PDF of solar irradiance
$v_{\omega i}$	The cut in wind speed of WT
$v_{\omega r}$	The rated wind speed of WT
$v_{\omega o}$	The cut out wind speed of WT
k, c	Shape and scale parameters of Weibull function
σ_d	The standard deviation of the load demand
μ_d	The mean deviation of the load demand
$\alpha_1, \alpha_2, \alpha_3, \alpha_4, \alpha_5$	The weight factors
ρ	Rate of interest on DG capital investment
T_{max}	Number of iterations
NP	Lifetime of the PV unit or the WT
NT	Number of branches
I_{max}	Maximum Allowable current in branches
Q_{WT}	Injected reactive power by wind turbine
NWT	Number of wind turbine
V_{min}	Minimum allowable voltage limit
V_{max}	Maximum allowable voltage limit
Q_{Grid}	Reactive power injected at slack bus
NPV	Number of PV units
$p_{d,i}^{max}$	The maximum limit of the selected interval i
$p_{d,i}^{min}$	The minimum limit of the selected interval i
v_z^{max}	The ending point of wind speed's interval at z -th scenario
v_z^{min}	The starting point of wind speed's interval at z -th scenario
G_m^{max}	The ending point of solar irradiance's interval at m -th scenario
G_m^{min}	The starting point of solar irradiance's interval at m -th scenario

Parameters and

Constants

G	Solar Irradiance
X_c	A certain irradiance point
G_{STD}	Standard environment solar irradiance (1000 W/m ²)
V_n	Voltage of the n -th bus
Γ	Gamma function
α, β	Parameters of the beta PDF
μ_s	Mean deviation of the solar irradiance for each time segment

Variables and

Functions

F	Multi-objective function
f_1	The objective function representing the normalized active total power losses
f_2	The objective function representing the normalized total voltage deviations
f_3	The objective function representing the normalized voltage stability index
f_4	The objective function representing the normalized total cost
f_5	The objective function representing the normalized total emission

References

1. Ganguly, S.; Sahoo, N.; Das, D. Recent advances on power distribution system planning: A state-of-the-art survey. *Energy Syst.* **2013**, *4*, 165–193. [[CrossRef](#)]
2. Sims, R.E.; Rogner, H.-H.; Gregory, K. Carbon emission and mitigation cost comparisons between fossil fuel, nuclear and renewable energy resources for electricity generation. *Energy Policy* **2003**, *31*, 1315–1326. [[CrossRef](#)]
3. Ehsan, A.; Yang, Q. Active distribution system reinforcement planning with EV charging stations—Part I: Uncertainty modeling and problem formulation. *IEEE Trans. Sustain. Energy* **2019**, *11*, 970–978. [[CrossRef](#)]
4. Cervantes, J.; Choobineh, F. Optimal sizing of a nonutility-scale solar power system and its battery storage. *Appl. Energy* **2018**, *216*, 105–115. [[CrossRef](#)]
5. Lai, C.S.; Jia, Y.; Lai, L.L.; Xu, Z.; McCulloch, M.D.; Wong, K.P. A comprehensive review on large-scale photovoltaic system with applications of electrical energy storage. *Renew. Sustain. Energy Rev.* **2017**, *78*, 439–451. [[CrossRef](#)]

6. Xavier, G.A.; Martins, J.H.; Monteiro, P.M.d.B.; Diniz, A.S.A.C.; Diniz, A.C. Simulation of distributed generation with photovoltaic microgrids—Case study in Brazil. *Energies* **2015**, *8*, 4003–4023. [[CrossRef](#)]
7. Weckx, S.; D'hulst, R.; Driesen, J. Locational pricing to mitigate voltage problems caused by high PV penetration. *Energies* **2015**, *8*, 4607–4628. [[CrossRef](#)]
8. Georgilakis, P.S.; Hatziargyriou, N.D. A review of power distribution planning in the modern power systems era: Models, methods and future research. *Electr. Power Syst. Res.* **2015**, *121*, 89–100. [[CrossRef](#)]
9. Gao, Y.; Liu, J.; Yang, J.; Liang, H.; Zhang, J. Multi-objective planning of multi-type distributed generation considering timing characteristics and environmental benefits. *Energies* **2014**, *7*, 6242–6257. [[CrossRef](#)]
10. El-Khattam, W.; Hegazy, Y.; Salama, M. An integrated distributed generation optimization model for distribution system planning. *IEEE Trans. Power Syst.* **2005**, *20*, 1158–1165. [[CrossRef](#)]
11. Liu, Z.; Wen, F.; Ledwich, G. Optimal siting and sizing of distributed generators in distribution systems considering uncertainties. *IEEE Trans. Power Deliv.* **2011**, *26*, 2541–2551. [[CrossRef](#)]
12. Shaaban, M.F.; El-Saadany, E. Accommodating high penetrations of PEVs and renewable DG considering uncertainties in distribution systems. *IEEE Trans. Power Syst.* **2013**, *29*, 259–270. [[CrossRef](#)]
13. Zeng, B.; Zhang, J.; Zhang, Y.; Yang, X.; Dong, J.; Liu, W. Active distribution system planning for low-carbon objective using cuckoo search algorithm. *J. Electr. Eng. Technol.* **2014**, *9*, 433–440. [[CrossRef](#)]
14. Peng, X.; Lin, L.; Zheng, W.; Liu, Y. Crisscross optimization algorithm and Monte Carlo simulation for solving optimal distributed generation allocation problem. *Energies* **2015**, *8*, 13641–13659. [[CrossRef](#)]
15. Esmaeili, M.; Sedighzadeh, M.; Esmaili, M. Multi-objective optimal reconfiguration and DG (Distributed Generation) power allocation in distribution networks using Big Bang-Big Crunch algorithm considering load uncertainty. *Energy* **2016**, *103*, 86–99. [[CrossRef](#)]
16. Santos, S.F.; Fitiwi, D.Z.; Bizuayehu, A.W.; Shafie-Khah, M.; Asensio, M.; Contreras, J.; Cabrita, C.M.P.; Catalao, J.P. Novel multi-stage stochastic DG investment planning with recourse. *IEEE Trans. Sustain. Energy* **2016**, *8*, 164–178. [[CrossRef](#)]
17. Kroposki, B.; Sen, P.K.; Malmedal, K. Optimum sizing and placement of distributed and renewable energy sources in electric power distribution systems. *IEEE Trans. Ind. Appl.* **2013**, *49*, 2741–2752. [[CrossRef](#)]
18. Baghaee, H.; Mirsalim, M.; Gharehpetian, G.; Talebi, H. Reliability/cost-based multi-objective Pareto optimal design of stand-alone wind/PV/FC generation microgrid system. *Energy* **2016**, *115*, 1022–1041. [[CrossRef](#)]
19. Saric, M.; Hivzievendic, J.; Konjic, T.; Ktena, A. Distributed generation allocation considering uncertainties. *Int. Trans. Electr. Energy Syst.* **2018**, *28*, e2585. [[CrossRef](#)]
20. Zhao, B.; Guo, C.; Cao, Y. A multiagent-based particle swarm optimization approach for optimal reactive power dispatch. *IEEE Trans. Power Syst.* **2005**, *20*, 1070–1078. [[CrossRef](#)]
21. Abdel-Fatah, S.; Ebeed, M.; Kamel, S. Optimal Reactive Power Dispatch Using Modified Sine Cosine Algorithm. In Proceedings of the 2019 International Conference on Innovative Trends in Computer Engineering (ITCE), Aswan, Egypt, 2–4 February 2019; pp. 510–514.
22. Sulaiman, M.; Rashid, M.M.; Aliman, O.; Mohamed, M.; Ahmad, A.; Bakar, M. Loss minimisation by optimal reactive power dispatch using cuckoo search algorithm. In Proceedings of the 3rd IET International Conference on Clean Energy and Technology (CEAT) 2014, Kuching, Malaysia, 24–26 November 2014.
23. Heidari, A.A.; Abbaspour, R.A.; Jordehi, A.R. Gaussian bare-bones water cycle algorithm for optimal reactive power dispatch in electrical power systems. *Appl. Soft Comput.* **2017**, *57*, 657–671. [[CrossRef](#)]
24. Li, Z.; Cao, Y.; Dai, L.V.; Yang, X.; Nguyen, T.T. Finding solutions for optimal reactive power dispatch problem by a novel improved antlion optimization algorithm. *Energies* **2019**, *12*, 2968. [[CrossRef](#)]
25. Villa-Acevedo, W.M.; López-Lezama, J.M.; Valencia-Velásquez, J.A. A novel constraint handling approach for the optimal reactive power dispatch problem. *Energies* **2018**, *11*, 2352. [[CrossRef](#)]
26. Abou El-Ela, A.; Kinawy, A.; El-Sehiemy, R.; Mouwafi, M. Optimal reactive power dispatch using ant colony optimization algorithm. *Electr. Eng.* **2011**, *93*, 103–116. [[CrossRef](#)]
27. Sakr, W.S.; El-Sehiemy, R.A.; Azmy, A.M. Adaptive differential evolution algorithm for efficient reactive power management. *Appl. Soft Comput.* **2017**, *53*, 336–351. [[CrossRef](#)]
28. Khazali, A.; Kalantar, M. Optimal reactive power dispatch based on harmony search algorithm. *Int. J. Electr. Power Energy Syst.* **2011**, *33*, 684–692. [[CrossRef](#)]
29. Dai, C.; Chen, W.; Zhu, Y.; Zhang, X. Seeker optimization algorithm for optimal reactive power dispatch. *IEEE Trans. Power Syst.* **2009**, *24*, 1218–1231.
30. Mandal, B.; Roy, P.K. Optimal reactive power dispatch using quasi-oppositional teaching learning based optimization. *Int. J. Electr. Power Energy Syst.* **2013**, *53*, 123–134. [[CrossRef](#)]
31. Faramarzi, A.; Heidarnejad, M.; Stephens, B.; Mirjalili, S. Equilibrium optimizer: A novel optimization algorithm. *Knowl.-Based Syst.* **2020**, *191*, 105190. [[CrossRef](#)]
32. Ramadan, A.; Ebeed, M.; Kamel, S.; Nasrat, L. Optimal power flow for distribution systems with uncertainty. In *Uncertainties in Modern Power Systems*; Elsevier: Amsterdam, The Netherlands, 2020; pp. 145–162.

33. Bastawy, M.; Ebeed, M.; Rashad, A.; Alghamdi, A.S.; Kamel, S. Micro-Grid Dynamic Economic Dispatch with Renewable Energy Resources Using Equilibrium Optimizer. In Proceedings of the 2020 IEEE Electric Power and Energy Conference (EPEC), Edmonton, AB, Canada, 9–10 November 2020; pp. 1–5.
34. Özkaya, H.; Yıldız, M.; Yıldız, A.R.; Bureerat, S.; Yıldız, B.S.; Sait, S.M. The equilibrium optimization algorithm and the response surface-based metamodel for optimal structural design of vehicle components. *Mater. Test.* **2020**, *62*, 492–496. [[CrossRef](#)]
35. Abdel-Basset, M.; Mohamed, R.; Mirjalili, S.; Chakraborty, R.K.; Ryan, M.J. Solar photovoltaic parameter estimation using an improved equilibrium optimizer. *Sol. Energy* **2020**, *209*, 694–708. [[CrossRef](#)]
36. Gampa, S.R.; Das, D. Optimum placement and sizing of DGs considering average hourly variations of load. *Int. J. Electr. Power Energy Syst.* **2015**, *66*, 25–40. [[CrossRef](#)]
37. Soroudi, A.; Aien, M.; Ehsan, M. A probabilistic modeling of photo voltaic modules and wind power generation impact on distribution networks. *IEEE Syst. J.* **2011**, *6*, 254–259. [[CrossRef](#)]
38. Mohseni-Bonab, S.M.; Rabiee, A. Optimal reactive power dispatch: A review, and a new stochastic voltage stability constrained multi-objective model at the presence of uncertain wind power generation. *IET Gener. Transm. Distrib.* **2017**, *11*, 815–829. [[CrossRef](#)]
39. Ebeed, M.; Alhejji, A.; Kamel, S.; Jurado, F. Solving the Optimal Reactive Power Dispatch Using Marine Predators Algorithm Considering the Uncertainties in Load and Wind-Solar Generation Systems. *Energies* **2020**, *13*, 4316. [[CrossRef](#)]
40. Hetzer, J.; David, C.Y.; Bhattarai, K. An economic dispatch model incorporating wind power. *IEEE Trans. Energy Convers.* **2008**, *23*, 603–611. [[CrossRef](#)]
41. Biswas, P.P.; Suganthan, P.N.; Mallipeddi, R.; Amaratunga, G.A.J. Optimal reactive power dispatch with uncertainties in load demand and renewable energy sources adopting scenario-based approach. *Appl. Soft Comput.* **2019**, *75*, 616–632. [[CrossRef](#)]
42. Atwa, Y.; El-Saadany, E.; Salama, M.; Seethapathy, R. Optimal renewable resources mix for distribution system energy loss minimization. *IEEE Trans. Power Syst.* **2009**, *25*, 360–370. [[CrossRef](#)]
43. Salameh, Z.M.; Borowy, B.S.; Amin, A.R. Photovoltaic module-site matching based on the capacity factors. *IEEE Trans. Energy Convers.* **1995**, *10*, 326–332. [[CrossRef](#)]
44. Liang, R.-H.; Liao, J.-H. A fuzzy-optimization approach for generation scheduling with wind and solar energy systems. *IEEE Trans. Power Syst.* **2007**, *22*, 1665–1674. [[CrossRef](#)]
45. Reddy, S.S.; Bijwe, P.; Abhyankar, A.R. Real-time economic dispatch considering renewable power generation variability and uncertainty over scheduling period. *IEEE Syst. J.* **2014**, *9*, 1440–1451. [[CrossRef](#)]
46. Mirjalili, S. SCA: A sine cosine algorithm for solving optimization problems. *Knowl.-Based Syst.* **2016**, *96*, 120–133. [[CrossRef](#)]
47. Eberhart, R.; Kennedy, J. A New Optimizer Using Particle Swarm Theory. In Proceedings of the Sixth International Symposium on Micro Machine and Human Science (MHS'95), Nagoya, Japan, 4–6 October 1995; pp. 39–43.
48. Mirjalili, S. The ant lion optimizer. *Adv. Eng. Softw.* **2015**, *83*, 80–98. [[CrossRef](#)]
49. Chandramohan, S.; Atturulu, N.; Devi, R.K.; Venkatesh, B. Operating cost minimization of a radial distribution system in a deregulated electricity market through reconfiguration using NSGA method. *Int. J. Electr. Power Energy Syst.* **2010**, *32*, 126–132. [[CrossRef](#)]
50. Pires, D.F.; Antunes, C.H.; Martins, A.G. NSGA-II with local search for a multi-objective reactive power compensation problem. *Int. J. Electr. Power Energy Syst.* **2012**, *43*, 313–324. [[CrossRef](#)]